HAL
open science

In-plane thermal diffusivity measurement of thin plates by the transient fin method

Yves Jannot, Alain Degiovanni, Arthur Aubert, François Lechleiter

To cite this version:

Yves Jannot, Alain Degiovanni, Arthur Aubert, François Lechleiter. In-plane thermal diffusivity measurement of thin plates by the transient fin method. Review of Scientific Instruments, 2018, 89 (10), 10.1063/1.5038401 . hal-01900573

HAL Id: hal-01900573

https://hal.univ-lorraine.fr/hal-01900573v1

Submitted on 22 Oct 2018

HAL is a multi-disciplinary open access archive for the deposit and dissemination of scientific research documents, whether they are published or not. The documents may come from teaching and research institutions in France or abroad, or from public or private research centers.

L'archive ouverte pluridisciplinaire **HAL**, est destinée au dépôt et à la diffusion de documents scientifiques de niveau recherche, publiés ou non, émanant des établissements d'enseignement et de recherche français ou étrangers, des laboratoires publics ou privés.

IN-PLANE THERMAL DIFFUSIVITY MEASUREMENT OF THIN PLATES BY THE TRANSIENT FIN METHOD

Yves Jannot[1], Alain Degiovanni[1,2], Arthur Aubert[3], François Lechleiter[4]
[1] Université de Lorraine, CNRS, LEMTA, F-54000 Nancy, France
[2] Université Internationale de Rabat, LERMA, 11100 Sala Al Jadida, Morocco
[3] ei.CESI, 54600 Villers-lès-Nancy, France
[4] CIMULEC, 57365 Ennery, France

ABSTRACT

The transient fin method has mainly be used for the measurement of in-plane thermal diffusivity of rather highly diffusive materials available under the form thin plates. This paper presents an extension of the method to low diffusivity materials such as plastics. An new analytical model is used in the real space, avoiding to make a Laplace transform of experimental temperatures recordings that may be inaccurate. Experiments carried on two materials under gas pressure varying from 10^{-2} mbar to 1 bar shows the great influence of heat conduction in the air surrounding the sample, leading to estimation errors that can reach 30% at atmospheric pressure. The experimental results also shows that accurate measurements can be achieved if the pressure is lower than 10^{-2} mbar.

INTRODUCTION

Knowledge of the thermal properties of materials available and used in thin plates is important in several fields including that of printed circuits. The support of the printed circuits is most often made of a plastic plate with a thickness of less than 1 mm. The conductivity in the direction Oz perpendicular to the plate is between $\lambda_z = 0.2\ \mathrm{W\ m^{-1}\ K^{-1}}$ and $\lambda_z = 2\ \mathrm{W\ m^{-1}\ K^{-1}}$ with factors of anisotropy $\frac{\lambda_x}{\lambda_z}$ and $\frac{\lambda_y}{\lambda_z}$ that can be up to 2.

To predict and limit the heating of the supports (and therefore of the circuits deposited therein), it is necessary to know precisely the in-plane thermal conductivities λ_x, λ_y and the normal thermal conductivity λ_z.

The thermal conductivity λ_z can be deduced from the thermal diffusivity a_z measured by the Flash method[1,2].

The measurement of the thermal conductivities λ_x or λ_y is a bit more complicated. The hot strip[3] and the hot disk[4,5] are based on the hypothesis that the sample can be considered as a semi-infinite medium but the thickness of the samples to be measured is less than 1 mm. Even if the measurement was realized on a time sufficiently short in order to respect the semi-infinite medium hypothesis, the measured temperature will be highly sensitive to the normal conductivity and poorly sensitive to the in-plane one since the hot disk sensor is several millimeters in diameter. Nevertheless, hot disk measurements have been already performed with finite thickness samples sandwiched between two insulating samples[4] , but this method is valid only if heat loss in the insulating samples is negligible compared with the total input of power to the sensor. Thus it enables thermal conductivity measurements of thin high conductivity materials such as copper, brass and aluminium, but it is not suited to thin low conductivity materials.

ACCEPTED PAPER

The hot wire[6,7] method cannot measure separately the in-plane and the normal conductivities in case of a thin plate.
The thermal conductivity λ_x can be deduced from the measurement of the thermal diffusivity a_x coupled with the measurement of the mass heat capacity by differential calorimetry.
Many measurement methods[8-17] derived from flash method and using infrared thermography were previously proposed to estimate in-plane thermal diffusivity of thin plates but they were applied to medium to high thermal diffusivity materials. The transient fin method[18] has already been used to measure the in-plane diffusivity of thin plates but only for highly conductive materials. The method is based on the recording of two temperatures and of the estimation of the transfer function between them in the Laplace space. It needs to realize the Laplace transformation of the experimental temperatures that may be not easy nor accurate.
We will show that the in-plane thermal diffusivity estimation of thin anisotropic materials may be biased by conduction heat transfer in the surrounding air for low diffusivity materials. This effect was not investigated in these references.
The problem of a bias due to heat conduction in air has already been faced by other authors[19-23]. Nevertheless, they only took into account the conduction in air in the Oz direction (normal direction, see figure 1) and did not investigate about the effect of the conduction in air in the Ox direction.
In this work we will present an extension of the transient fin method to low diffusivity materials such as plaster or resin based materials taking into account the conduction heat transfer occurring in the surrounding air. We will show that in our device, the conduction in air in the Oz direction is quasi perfectly taken into account by the convection heat transfer coefficient and that the bias is only due to the conduction in air in the Ox direction.
Moreover, a new analytical model enabling the estimation in the real space is developed: it avoids to make a possibly inaccurate Laplace transform of the experimental data as previously done[18].

MODEL

The scheme of the sample used in the transient fin method is given in figure 1. It is considered that the sample is initially at a uniform temperature and equal to the temperature T_a of the ambient air. A heat flow rate $\varphi_0(t)$ is applied on one of its ends, the intensity and the time variations of which are not required to be known. The temporal evolutions of the temperatures T_1 and T_2 are measured at respective distances x_1 and x_2 of the heated edge by electrical resistance variation of a metallic strip, by bonded thermocouples or by an IR camera. These measurements, combined with a modeling of heat transfer, make it possible to deduce the thermal diffusivity a_x.
This model is based on the following hypotheses:

- The thermal gradient in the direction of thickness e is negligible (thin system), which is verified if $Bi < 0.1$, where $Bi = \frac{he}{\lambda_z}$ is the Biot number.
- The plate is long enough so that it can be considered as a semi-infinite medium for the duration of the measurement.

ACCEPTED PAPER

- The plate is wide enough so that the edge effects in the direction Oy have no effect at the center of the plate.
- Heat transfer by conduction in the air is negligible
- The global heat transfer coefficient is the same on the two faces (upper and lower).

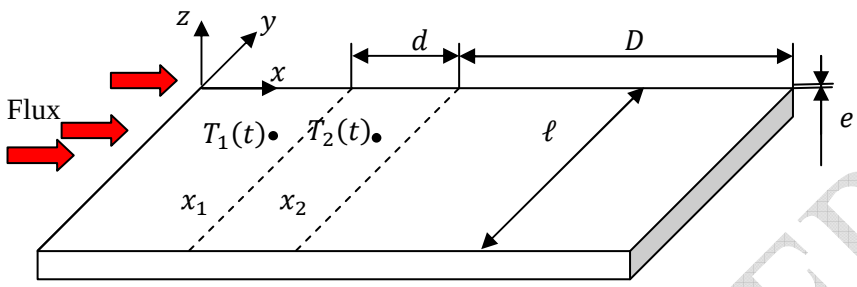

Figure 1: Diagram of the principle of the transient fin method

It has been demonstrated[24] that this last hypothesis has no influence on the estimation result considering the flash method as an example.

With these hypotheses, the system of equations describing the transfer is written as:

$$\frac{\partial^2 T}{\partial x^2} - \frac{h\,P_e}{\lambda_x S}(T - T_a) = \frac{1}{a_x}\frac{\partial T}{\partial t} \quad (1)$$

With: $T(x, t = 0) = T_a$ (2)

$T(x_1, t) = T_1$ (3)

$T(x \to \infty, t) = T_a$ (4)

And where: $P_e = 2(e + \ell)$ is the perimeter.

$S = e\ell$ is area of the section associated to the heat flow rate

Given: $\bar{T} = T - T_a$ and designating $\theta(x, p)$ the Laplace transform of $\bar{T}(x, t)$, these equations become:

$$\frac{d^2\theta}{dx^2} - \left(\frac{p}{a_x} + \frac{h\,P_e}{\lambda_x S}\right)\theta = 0 \quad (5)$$

The general solution is written in the form: $\theta(x, p) = A\,exp(-qx) + B\,exp(qx)$ (6)

Where: $q = \sqrt{\frac{p}{a_x} + \frac{hP_e}{\lambda_x S}}$ (7)

The semi-infinite medium hypothesis leads to: $B = 0$

The solution thus takes the form: $\theta(x, p) = A\,exp(-qx)$ (8)

In particular : $\theta_1(p) = A\,exp(-qx_1)$ and $\theta_2(p) = A\,exp(-qx_2)$ (9)

Hence: $\theta_2(p) = \theta_1(p)\,exp(-qd)$ (10)

Where: $d = x_2 - x_1$

Thus θ_2 depends only on θ_1 and the following parameters: p, $\frac{d^2}{a_x}$ and $\frac{hP_e d^2}{\lambda_x S}$

And we can write it in real space as:

$\bar{T}_2(t) = \bar{T}_1(t) \otimes F(t)$ (11)

Where $F(t) = L^{-1}[H(p)]$ is the inverse Laplace transform of $H(p)$.

With: $H(p) = exp(-qd)$ (12)

ACCEPTED PAPER

Finally: $F(t) = \frac{1}{2}\frac{d}{\sqrt{\pi t^3 a_x}} exp\left(-\frac{hP_e}{\rho c S}t - \frac{1}{4}\frac{d^2}{a_x t}\right)$ (13)

PARAMETERS ESTIMATION METHOD

This modeling of the system makes it possible to obtain the analytical expression of the transfer function of the system $F(t)$ between the input $\bar{T}_1(t)$ and the output $\bar{T}_2(t)$. This transfer function depends only on t, a_x (thermal diffusivity) and h (convection-radiation transfer coefficient).

The two parameters a_x and h are estimated by minimizing the sum of the quadratic deviations between the experimental curve $\bar{T}_{2exp}(t)$ and the model curve calculated by an equation of type $\bar{T}_{2mod}(t) = \bar{T}_{1exp}(t) \otimes F(t, a_x, h)$ where $\bar{T}_{1exp}(t)$ is considered as an input data of the problem.

The function $F(t)$ is computed by equation (13). The minimization of the sum of the quadratic deviations is performed by the Levenberg-Marquart algorithm[25].

The reduced sensitivities of $\bar{T}_2(t)$ to a parameter X is defined by[26]: $X\frac{\partial \bar{T}_2}{\partial X}$. We have calculated the reduced sensitivities of $\bar{T}_2(t)$ to the parameters a and h to verify that these two parameters can be estimated simultaneously from a unique experiment.

The reduced sensitivity has been calculated numerically by the approximation justified by Maillet et al[27]:

$$\frac{\partial \bar{T}_2}{\partial X} = \bar{T}_1(t) \otimes \frac{\partial F}{\partial X}(t, a_x, h) \quad (14)$$

The calculation was realized numerically, for example:

$$a_x \frac{\partial \bar{T}_2}{\partial a_x} = a_x \frac{\bar{T}_{1exp}(t) \otimes F(t, 1.001 \times a_x, h) - \bar{T}_{1exp}(t) \otimes F(t, a_x, h)}{0.001 \times a_x} \quad (15)$$

An example of the calculated sensitivities is represented in figure 2. The two reduced sensitivities are not proportional so one can conclude that the two parameters a and h can be estimated separately[10].

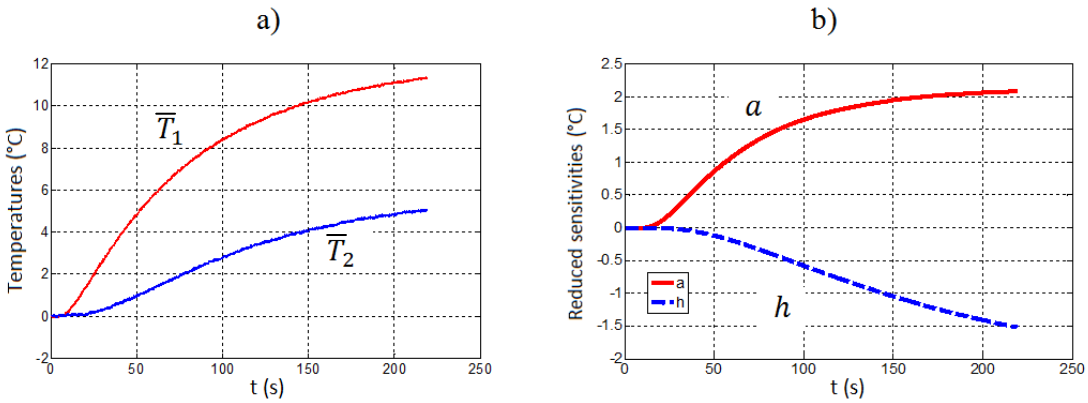

Figure 2: a) Temperature curves $\bar{T}_1(t)$ and $\bar{T}_2(t)$; b) Reduced sensitivities of $\bar{T}_2(t)$ to a_x and h for a resin : $a_x = 3.2 \times 10^{-7}\ m^2 s^{-1}$; $h = 7\ \mathrm{W\,m^{-2}K^{-1}}$; $e = 0{,}8\ mm$.

The calculation of the reduced sensitivities for several values of the heat transfer coefficient h and of the sample thickness e lead to the following conclusions:

- The sensitivity to h decreases if the thickness e of the plate increases: it is therefore not necessary to work with plates that are too thin, especially if the thermal diffusivity

is low.

- The sensitivity to h decreases if the value of h decreases: we will therefore work under vacuum whenever possible, which will also make it possible to limit the conductive transfer in the air neglected in the model.

EXPERIMENTAL SETUP

The experiments were carried on two materials used as PCB's support:

- Megtron (thickness $e = 0.8$ mm)
- Arlon 35N (thicknesses $e = 0.6$ mm and $e = 0.8$ mm)

Samples with dimensions 100 x 100 mm^2 were cut in the three plates and three cooper strips were deposited on one of their surfaces. The thickness of the strips is 17 µm and the width is 80 µm.

A scheme and a view of a sample are presented in figure 3 and a view of the experimental setup is presented in figure 4. Starting from a thermal equilibrium state, a heat flow rate $\varphi_0(t)$ is produced by passing a current with intensity I_0 through the resistive strip S_0. This current is produced by a current generator. To avoid edge effects, a rather large sample (square of 10 cm side) was used in our experiments. The values of x_1 and x_2 must be large enough so that the uncertainty about their difference d is small ($x_1 = 5$ mm and $x_2 = 10$ mm in our experiments). The distance D (see Figure 1) must also be sufficiently large for the semi-infinite medium hypothesis to remain valid for a sufficiently long time, its value is 40 mm for our samples. An electrical current with a low and constant intensity $I_1 = I_2 = 0.05A$ is produced by a current generator and passes through the two strips S_1 and S_2. The transient values of their resistances R_1 and R_2 are deduced from the measurement of the electrical tensions U_1 and U_2 realized with a ALMEMO 2890-9 with a recording time step of 0.1s (acquisition frequency of 10 Hz). The temperatures rises $\bar{T}_i(t) = T_i(t) - T_i(t = 0)$ can then be deduced by:

$$\bar{T}_i(t) = \frac{1}{\alpha}\frac{R_i(t) - R_i(t=0)}{R_i(t=0)} \tag{16}$$

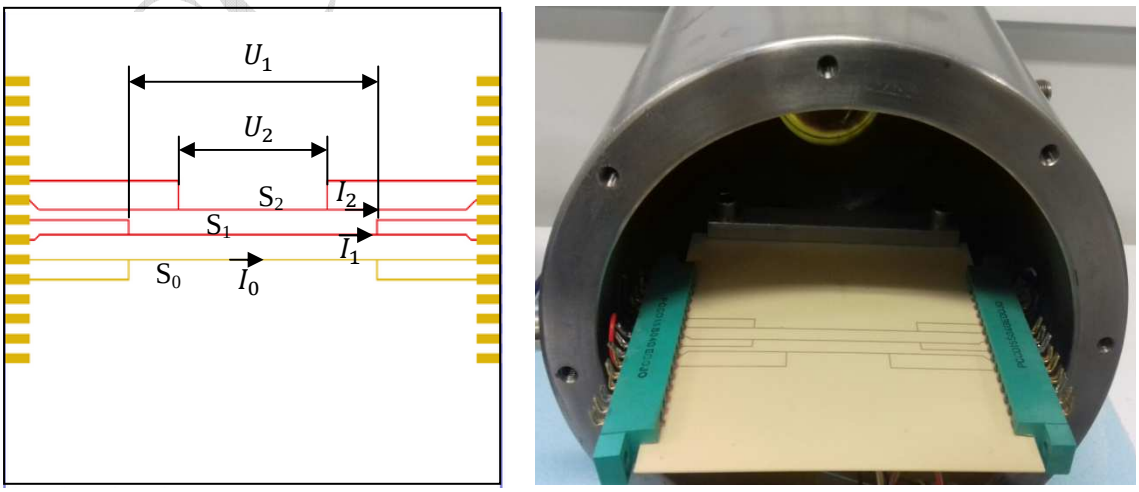

Figure 3: Scheme of a sample and view of the vacuum vessel

.

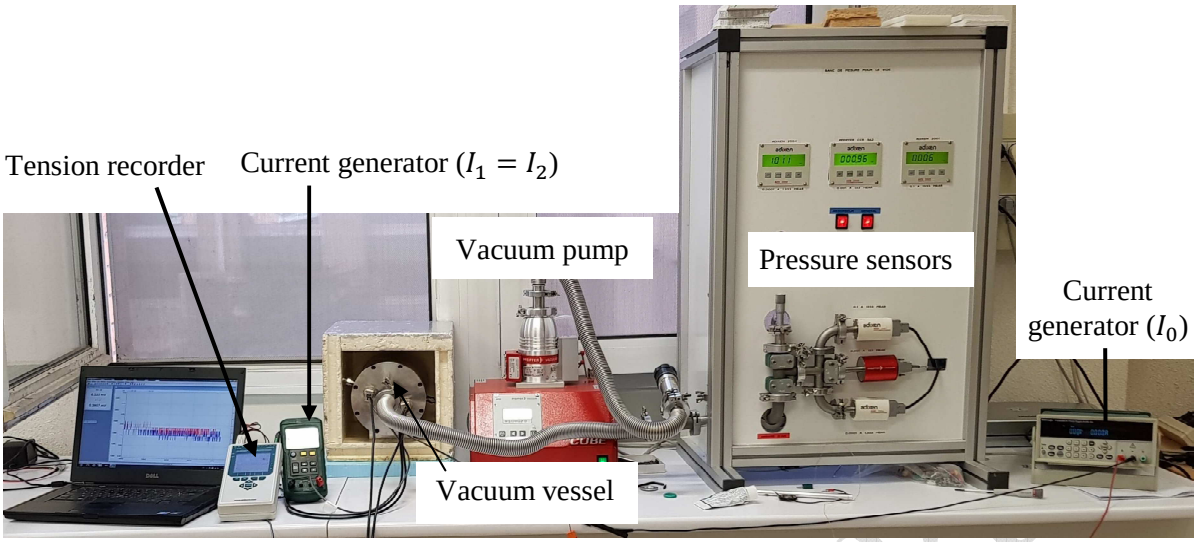

Figure 4 : View of the experimental set up

It should be noted that in this type of method, the measurement of two quantities proportional to the temperatures (with the same coefficient of proportionality) is sufficient. In our case, the two strips have the same temperature coefficient α since they have the same composition. Thus, it is not necessary to know the value of α that is a key advantage. It is not either necessary to know the transient values of the heat flux that is another benefit.

The reduced sensitivity study showed that the sensitivity to h decreases with the value of h, so it is advantageous to minimize this value. For this reason the samples has been placed in a vacuum vessel where the pressure can be controlled from 10^{-2} mbar to 1 bar.

The mass thermal capacities c of Arlon and Megtron have been measured with a SETARAM µdSc3 differential calorimeter. The measured values of c (J kg^{-1} °C^{-1}) can be represented by a precision better than 0.5% by the following formulas :

$$c_{Arlon} = 124.16 + 2.614\,T \quad (17)$$

$$c_{Megtron} = 216.92 + 2.462\,T \quad (18)$$

Where T is the temperature (K)

Their densities have been deduced from measurement of the dimensions and weighting, the values for Arlon and Megtron are respectively 1930 kg m^{-3} and 1620 kg m^{-3}.

These values enable the calculation of the thermal conductivity from the thermal diffusivities by: $\lambda_x = a_x\,\rho c$.

RESULTS AND DISCUSSION

As an example, figure 5.a) presents two experimental curves $\bar{T}_{1exp}(t)$ and $\bar{T}_{2exp}(t)$ and figure 5.b) presents the experimental and modeled curves $\bar{T}_{2exp}(t)$ and $\bar{T}_{2mod}(t)$ both with the estimation residues $(\bar{T}_{2exp} - \bar{T}_{2mod})$.

Figures 6 presents the estimated values of the thermal conductivities of Arlon for two different plate thicknesses. The following remarks can be made:

- It is first remarkable that at low pressure the thermal conductivities of the two plates are

identical and equal to 0.6 W m^{-1} K^{-1}

- The estimation error made with a measurement under a gas pressure greater than 1 mbar is more than 50%
- This error increases if the plate thickness decreases.

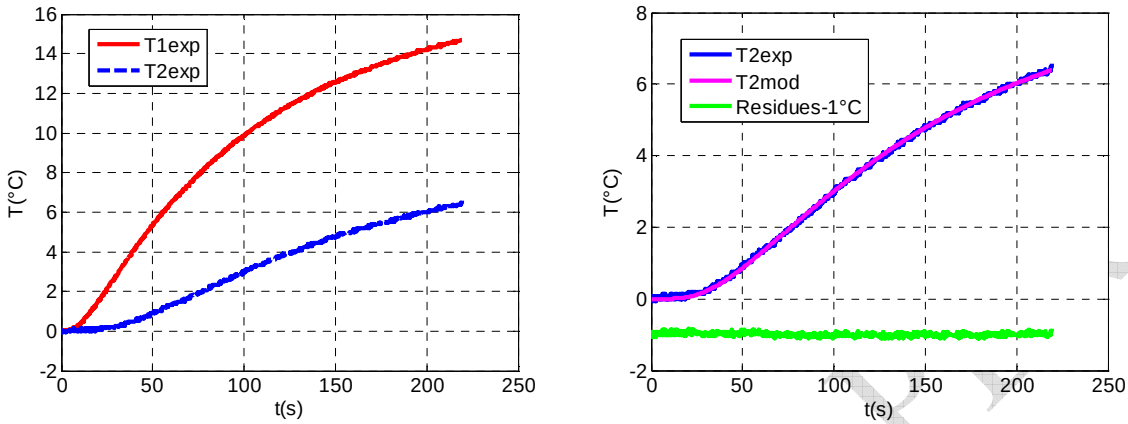

Figure 5: a) Experimental temperatures $\bar{T}_{1exp}$ and $\bar{T}_{2exp}$ obtained with Arlon; b) experimental and model temperature $\bar{T}_{2exp}$ and $\bar{T}_{2mod}$ with estimation residues (-1°C)

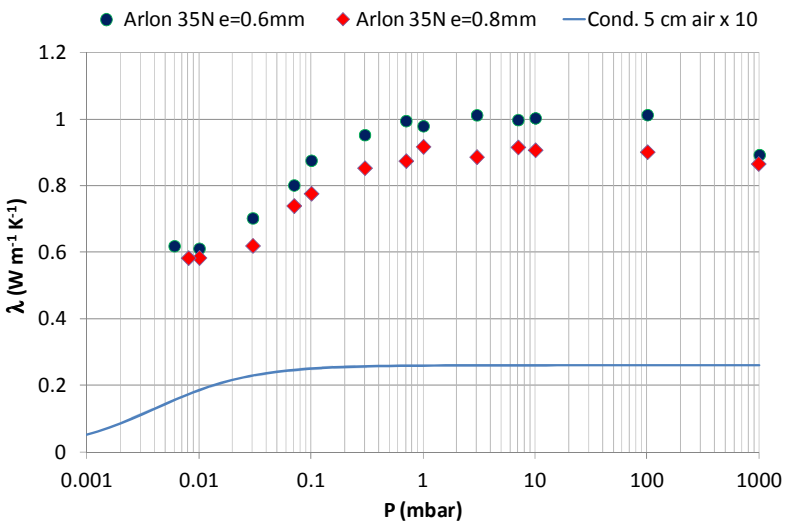

Figure 6: Thermal conductivity of Arlon at 24°C for two different plate thicknesses and thermal conductivity of air ×10 (5 cm thickness)

To support further explanations to these observations, we have schematically represented in figure 7 all the heat transfers occurring in the sample:

- A conduction heat flux from the heating element to the measuring strips
- A radiation heat flux with a coefficient h_r from the surface of the sample to the environment
- A convection heat flux (normal to the surface) with a coefficient h_c that can be seen as a conduction heat flux through the air boundary layer between the surface of the sample and the isothermal surface $T = T_a$
- A conduction heat flux (parallel to the surface) through the same air boundary layer.
-

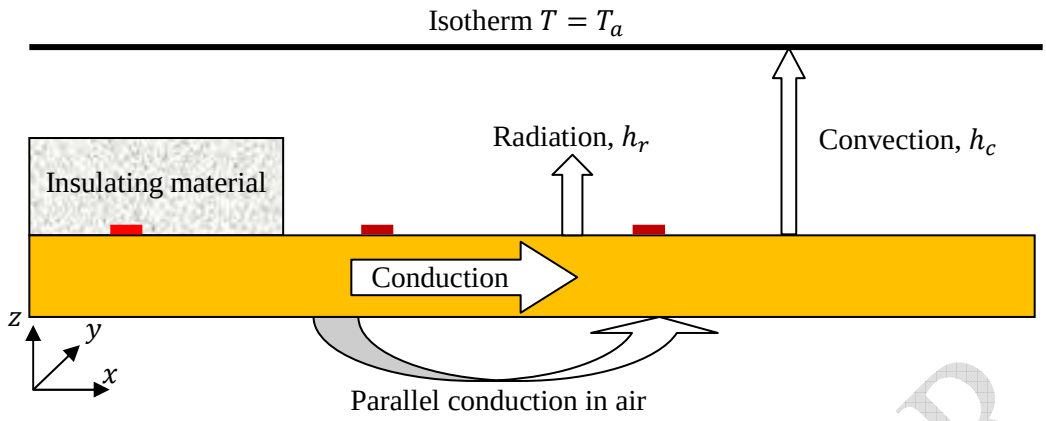

Figure 7: Schematic representation of the heat fluxes

The developed model takes into account radiation and convection with a global heat transfer coefficient $h = h_c + h_r$ but the conduction parallel to the surface in the air is not taken into account.

The thermal conductivity of a layer with a characteristic length L (thickness or diameter) can been calculated by[28]:

$$\lambda_{air} = \frac{\lambda_0}{1+\frac{6.81\times10^{-5}\,T_a}{P\,L}} \tag{19}$$

With :

$\lambda_0 = 0.026\ \mathrm{W\ m^{-1}\ K^{-1}}$

T_a air temperature (K)

P air pressure (Pa)

L characteristic length (m)

As an example, the thermal conductivity of air (for a 5 cm thickness layer, corresponding to the magnitude order of the distance between the sample and the wall of the enclosure) as a function of the pressure has been represented on figure 6. At low pressure the thermal conductivity of air decreases so that the heat flux by-passing by conduction in the surrounding air becomes negligible. Moreover, one can see on figure 6 that the decreasing of the estimated thermal conductivity of the sample and the thermal conductivity of air exhibit the same pattern. Especially between 1 and 100 mbar, the thermal conductivity of air no longer varies so that the by-passing parallel heat flux remains constant and thus the estimated value of the sample thermal conductivity does not vary. Nevertheless, the decreasing of the sample thermal conductivity at pressure greater that 100 mbar cannot be explained by the variation of the thermal conductivity of air.

The increasing of the estimation error on thermal conductivity if the plate thickness decreases can be explained by comparing the heat flux passing through the sample and the heat flux by-passing by the surrounding air. The second one does not depend on the plate thickness since the first one decreases if the plate thickness decreases. The estimation of the thermal conductivity is more accurate if the second one is low compared to the first one, thus it is better to use a thicker plate if possible.

Figure 8 represents the estimated conductivities of Megtron at respectively 24°C and 60°C. It shows that the thermal conductivity of Megtron is quite independent on temperature in

ACCEPTED PAPER

this interval. The decreasing of the estimated thermal conductivity for pressure greater than 100 mbar may be explained by the increasing of the convection heat transfer coefficient, reducing the boundary layer thickness in which a parallel heat flux is transferred by conduction in the surrounding air, as illustrated in figure 7.

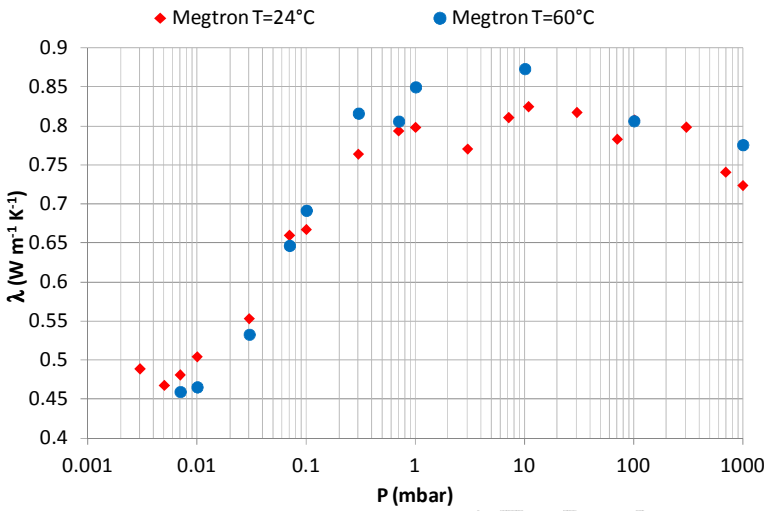

Figure 8: Thermal conductivity λ_x of Megtron for two different temperatures

Figure 9 represents the estimated heat transfer coefficient at respectively 24°C and 60°C for measurements realized on a Megtron plate. The difference between the values can be explained considering the radiation heat transfer.

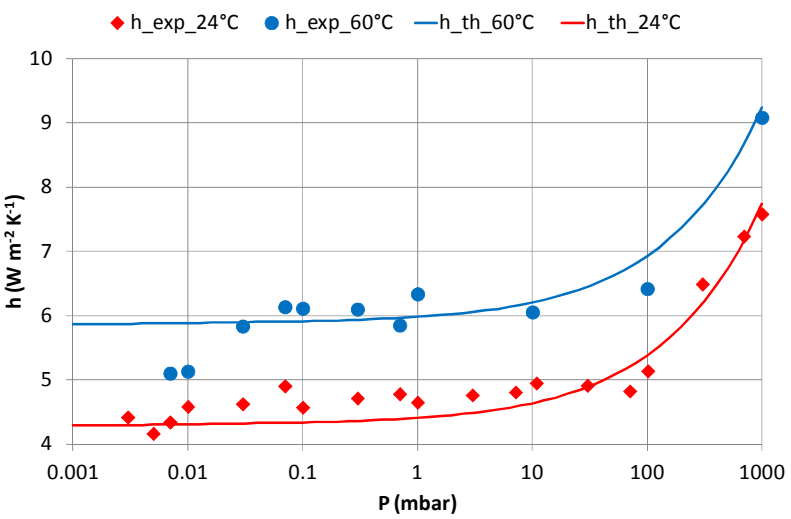

Figure 9: Experimental and theoretical heat transfer coefficient for Megtron at two different temperatures.

The convection heat transfer coefficient h_c in laminar regime can be calculated using[29]:

$$Nu_\ell = 0.53\ (Gr\ Pr)^{1/4} \tag{20}$$

Where: $$Gr\ Pr = \frac{\rho\ c\ g\ \ \beta\ \Delta T\ \ell^3}{\lambda\ \mu} \tag{21}$$

With: $$\rho = \frac{P}{287\ T} \tag{22}$$

T sample temperature (K)

$c = 1000\ \mathrm{J\ kg^{-1}\ K^{-1}}$

μ given by the curve on figure 10 from Schaller and Buffat[30]

$\Delta T = T - T_a$, where T_a is the ambient air temperature.

The value $\Delta T = 2\ °C$ has been used for the curve represented in figure 9.

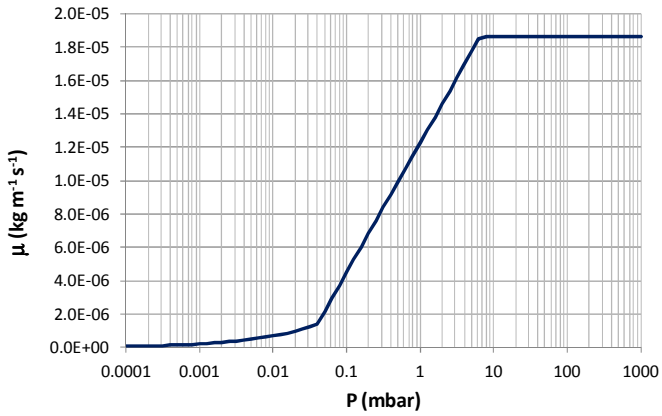

Figure 10: Air viscosity as a function of pressure[30]

Concerning the radiation heat transfer, the heat flux was linearized as:

$$\phi = \varepsilon\sigma\left(T^4 - {T_a}^4\right) \approx 4\varepsilon\sigma\, T^3 (T - T_a) \qquad (23)$$

With:

ε emissivity

σ Stephan-Boltzmann constant

The radiation heat transfer coefficient can be expressed as: $h_r = 4\varepsilon\sigma\, T^3$ (24)

And the global heat transfer coefficient h may be finally calculated by : $h = h_c + h_r$ (25)

Using a realistic value $\varepsilon = 0.7$ in relation (24), one can notice in figure 9 a good agreement between the experimental and the theoretical curves. In particular, the convective heat transfer coefficient becomes negligible if the pressure is lower than 100 mbar (contrarily to the thermal conductivity of air that is negligible only if the pressure is lower than 10^{-2} mbar for a millimetric thickness air layer).

The experimental results indicates an estimation bias due to conduction in the surrounding air. According to several previous papers[19-23] this bias may be due to conduction in air in the normal (Oz) direction but we think that it is mainly due to the conduction in air but in the Ox direction. To study the effect of conduction in air in the two directions on the estimated values of the thermal diffusivity of the sample to be characterized, we have realized a 2D simulation with COMSOL considering that the surface sample is surrounded by an air layer with a thickness e_air and also exchange by radiation with a coefficient h_r as represented on the figure 11.

To be more realistic, the air boundary layer thickness e_air (in which conduction heat transfer occurs) has be chosen as the minimum value between:

- The limit layer thickness calculated by $e_air_{lim} = \frac{\lambda_air_x}{h_c}$ where h_c has been calculated as previously explained in our paper.

ACCEPTED PAPER

- A maximum value e_air_{max} depending on vessel dimension.

The following values of the parameters have been considered for the simulations:

- $h_r = 4\ \mathrm{W\ m^{-2} K^{-1}}$
- $\lambda_x = 0.5\ \mathrm{W\ m^{-1}\ K^{-1}}$, $\rho c = 1.5 \times 10^6\ \mathrm{J\ m^{-3}\ K^{-1}}$
- $\lambda_air_z = 0.026\ \mathrm{W\ m^{-1}\ K^{-1}}$

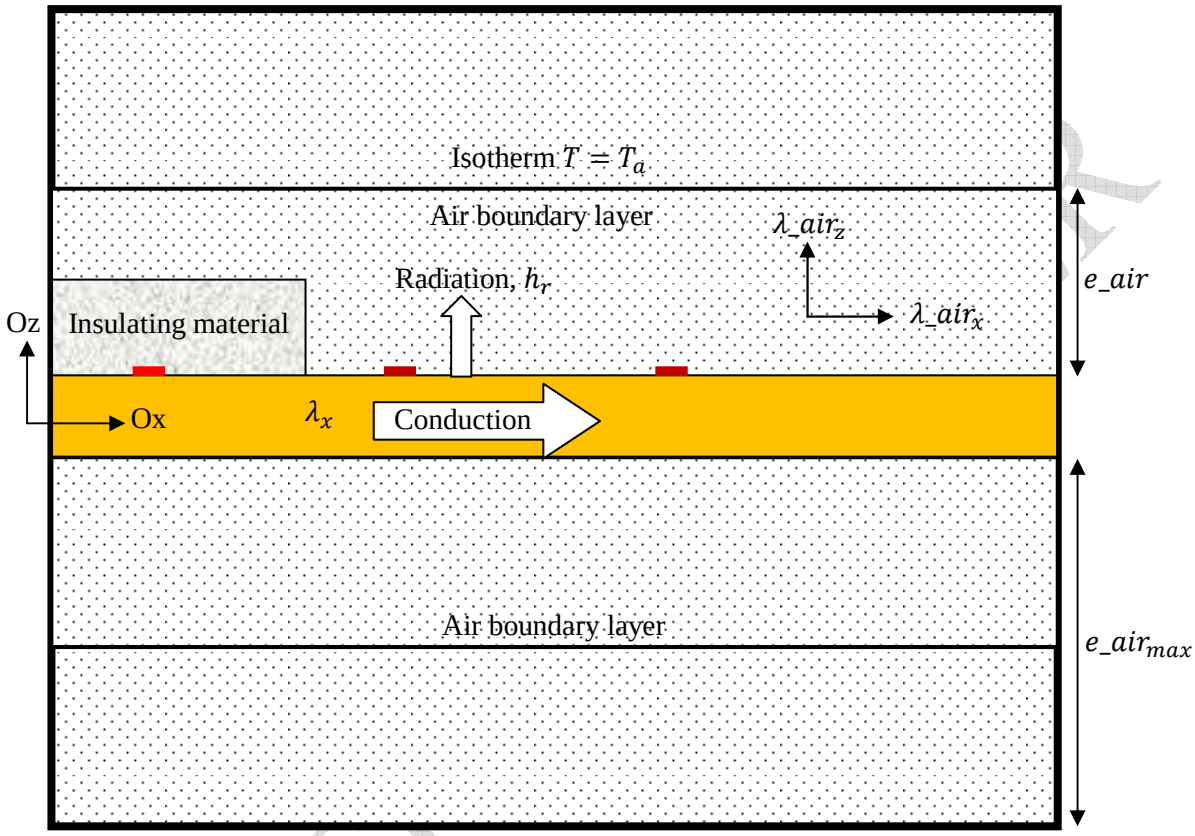

Figure 11 : Schematic representation of the system modeled with COMSOL

The air pressure have been varied between 10^{-4} mbar and 1 bar. The thermal conductivity of air inside the vessel has been calculated by relation (19) with $L = e_air_{max}$

For each pressure two simulations were realized to evaluate separately the influence of the conduction in air in the Ox direction and in the Oz direction:

- one with $\lambda_air_x = 0.026\ \mathrm{W\ m^{-1}\ K^{-1}}$
- another one with $\lambda_air_x = 0\ \mathrm{W\ m^{-1}\ K^{-1}}$

Then these simulated curves were considered as numerical experiments and the estimation process was applied to estimate the values of the thermal conductivity λ_x and of the global heat transfer coefficient h. The estimated values of the thermal conductivity λ_x of the sample and of the global heat transfer coefficient h are reported on figure 12 and figure 13.

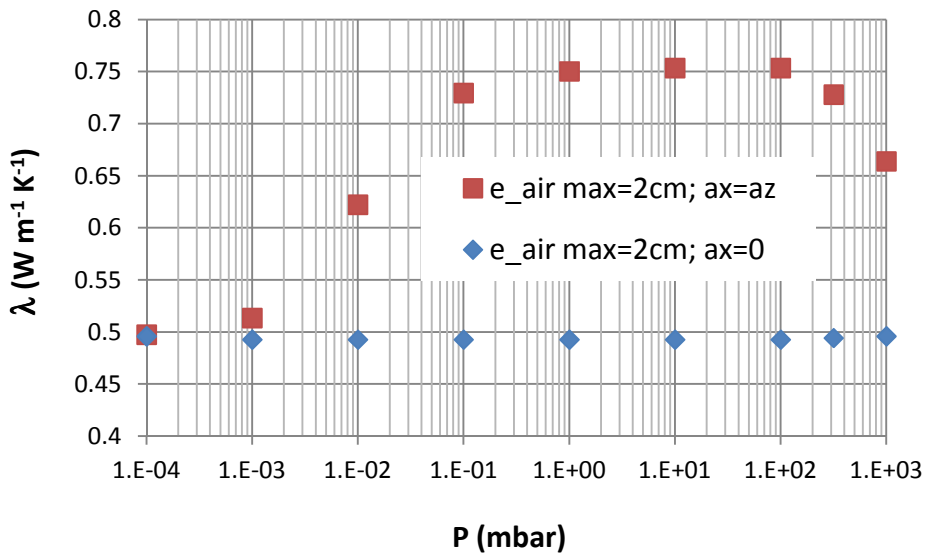

Figure 12 : Estimated values of the sample thermal conductivity λ_x using a COMSOL simulation taking into account conduction in air

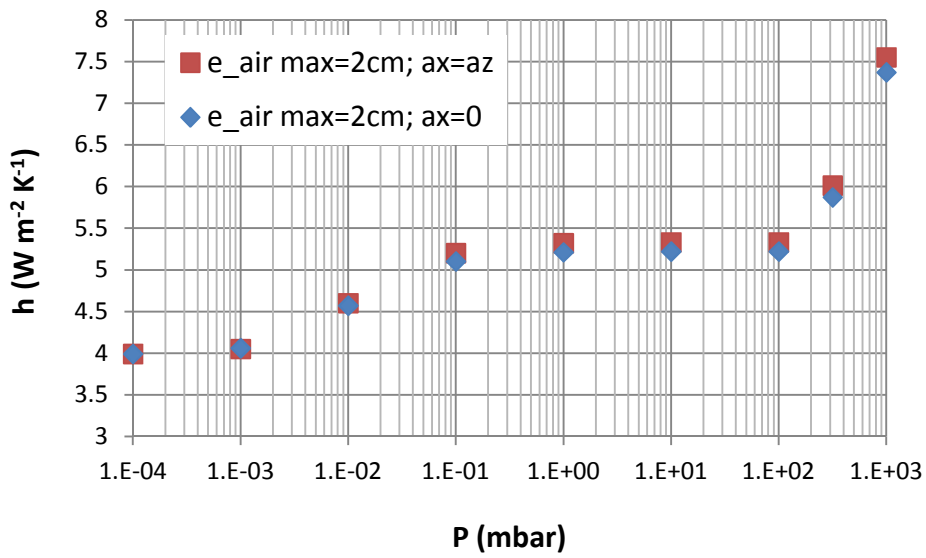

Figure 13 : Estimated values of the global heat transfer coefficient h using a COMSOL simulation taking into account conduction in air

Figure 12 shows that the estimation bias is only due to the conductivity in air in the Ox direction since the estimated value of λ_x is constant and equal to the value used for the simulation if the conduction in the Ox direction is not taken into account (case $a_x = \lambda_x = 0$). It is also remarkable that the variations of the estimated values of λ_x as a function of the pressure are quite similar to those obtained from an experimental curve in the case $\lambda_air_x = \lambda_air_z$ (cf. figure 6 and 8).

The values of the heat transfer coefficient estimated from data simulated with or without conduction in air in the Ox direction are rather identical (cf. figure 13). In both cases it has been verified for all the pressures that the estimated value is very close to: $h_r + \frac{\lambda_air_x}{e_air}$.

This mean that the conduction in air in the Oz direction is perfectly taken into account by a

convective heat transfer coefficient $h_c = \frac{\lambda_air_x}{e_air}$.

Considering that:

- the estimated value of h is very closed to the value calculated by $h = h_r + \frac{\lambda_air_x}{e_air}$
- the estimation residues are very low and centered on zero value as shown in figure (14),

one can say that the effect of the conduction in air in the Ox direction is perfectly correlated to the effect of λ_x. Thus this last parameter could not be estimated separately even if a model taking into account the conduction in air in the Ox direction is used for the estimation. The only way to realize an unbiased estimation is thus to realize the measurement under a low air pressure so that the conduction in air becomes negligible.

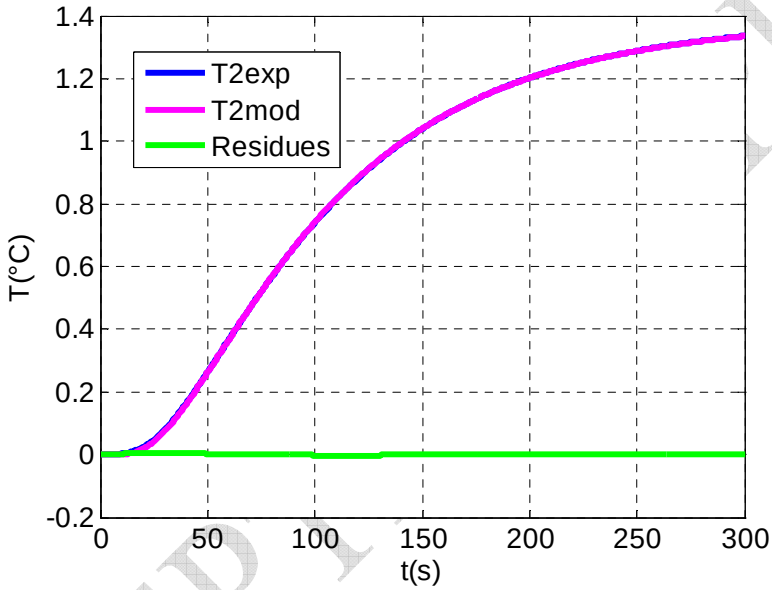

Figure 14: Temperatures simulated with COMSOL taking into account conductivity in air in the two directions, simulated curves with the estimated parameters and estimation residues.

Pressure increasing could be considered as a good solution since it decreases the influence of the conduction in the air. Nevertheless, pressure increasing make the heat transfer coefficient h increasing so that the sensitivity of T_2 to h can become greater than the sensitivity to the sample thermal conductivity. Moreover the two sensitivities are also more correlated when h increases. In conclusion, pressure increasing would not lead to an accurate estimation of the sample thermal conductivity λ_x.

CONCLUSION

The transient fin method previously used for in-plane high thermal diffusivity measurement has been extended to low diffusivity measurement such as resins for PCB support. Numerical simulation have shown that the conduction heat transfer in the air in the direction parallel to the plate heat leads to a biased estimation of the in-plane thermal diffusivity a_x of the plate. It has also been shown that accurate values of a_x can be estimated if the measurement are carried on in a vacuum enclosure with a pressure lower than 10^{-2} mbar. A

new analytical expression of the transfer function between two temperatures has been established in the real time space, it is thus no longer necessary to realize a Laplace transform of the experimental temperatures as previously requested.

NOMENCLATURE

a_{xy}	In-plane thermal diffusivity	$m^2\ s^{-1}$
Bi	Biot number	
c	Specific heat	$J\ kg^{-1}\ K^{-1}$
d	Distance between the two measuring strips	m
e	Sample thickness	m
F	Transfer function in the real space	
H	Transfer function in the Laplace space	
h	Global heat transfer coefficient	$W\ m^{-2}\ K^{-1}$
h_c	Convection heat transfer coefficient	$W\ m^{-2}\ K^{-1}$
h_r	Radiation heat transfer coefficient	$W\ m^{-2}\ K^{-1}$
I_i	Electrical current intensity in the ith strip	A
L	Characteristic length	m
ℓ	Sample width	m
Nu	Nusselt number	
P_e	Perimeter	m
P	Air pressure	Pa
Pr	Prandtl number	
p	Laplace parameter	s^{-1}
R_i	Electrical resistance of the ith strip	Ω
S	Sample section	m^2
T_a	Air temperature	K
T_i	Plate temperature at a distance x_i from the heating strip	K
$\bar{T}_i$	Reduced temperature $T_i - T_a$	
x_i	Distance from the heating strip	m
U_i	Electrical tension on the ith strip	V
α	Temperature coefficient of the electrical resistance	K^{-1}
ε	Emissivity	
φ_0	Heat flow rate	W
λ_{air}	Thermal conductivity of a L thickness air layer	$W\ m^{-1}\ K^{-1}$
λ_0	Thermal conductivity of an unlimited air layer	$W\ m^{-1}\ K^{-1}$
λ_x	In-plane thermal conductivity in the direction Ox	$W\ m^{-1}\ K^{-1}$
λ_z	Normal thermal conductivity	$W\ m^{-1}\ K^{-1}$
μ	Viscosity	$kg\ m^{-1}\ s^{-1}$
σ	Stephan-Boltzmann constant	
ρ	Sample density	$kg\ m^{-3}$
θ_i	Laplace transform of the temperature $\bar{T}_i$	

ACCEPTED PAPER

REFERENCES

[1] Degiovanni A. and Laurent A., "Une nouvelle technique d'identification de la diffusivité thermique pour la méthode flash", Revue de Physique Appliquée, **21**, 229–237 (1986).

[2] Parker W.J., Jenkins R.J. and Butler C.P., "Flash method of determining thermal diffusivity, heat capacity and thermal conductivity", Journal of Applied Physics, **32**, 9, 1679–1684 (1961).

[3] Gustafsson S.E., "Transient hot strip techniques for measuring thermal conductivity and thermal diffusivity", The Rigaku Journal, **4**, 1–2, 16–28 (1987).

[4] Gustavsson M., Karawacki E. and Gustafsson S.E., "Thermal conductivity, thermal diffusivity and specific heat of thin samples from transient measurement with Hot Disk sensors", Review of Scientific Instruments, **65** (1994).

[5] Bohac V., Gustavsson M.K., Kubicar L. and Gustafsson S.E., "Parameter estimations for measurements of thermal transport properties with the hot disk thermal constants analyzer " Rev. Sci. Instrum., **71**, 2452–2455 (2000).

[6] Andersson P., "Thermal conductivity of some rubbers under pressure by the transient hot-wire method", J. Appl. Phys., **47**, 2424–6 (1976).

[7] Zhang X., Degiovanni A. and Maillet D., "Hot-wire measurement of thermal conductivity of solids: a new approach", High Temp. High Press., **25**, 577–84 (1993).

[8] Welch, C. S., Heath, D. M., & Winfree, W. P., "Remote measurement of in - plane diffusivity components in plates", Journal of applied physics, **61**(3), 895-898 (1987).

[9] Okamoto Y., Watanabe S., Ogata K., Hiramatsu K., Miyazaki H., & Morimoto J., "Proposal of novel measurement method for thermal diffusivity from infrared thermal movie", Japanese Journal of Applied Physics, **56**(5), 056601 (2017).

[10] Miettinen L., Kekäläinen P., Merikoski J., Myllys M., & Timonen J., "In-plane thermal diffusivity measurement of thin samples using a transient fin model and infrared thermography", International Journal of Thermophysics, **29**(4), 1422-1438 (2008).

[11] Krapez J. C., Spagnolo L., Frieß M., Maier H. P., & Neuer G., " Measurement of inplane diffusivity in non-homogeneous slabs by applying flash thermography", International Journal of Thermal Sciences, **43**(10), 967-977 (2004).

[12] Bamford M., Florian M., Vignoles G. L., Batsale J. C., Cairo C. A. A., & Maillé L., "Global and local characterization of the thermal diffusivities of SiCf/SiC composites with infrared thermography and flash method", Composites Science and Technology, **69** (7-8),1131-1141 (2009).

[13] Ruffio E., Saury D., & Petit D., "Improvement and comparison of some estimators dedicated to thermal diffusivity estimation of orthotropic materials with the 3D-flash method", International Journal of Heat and Mass Transfer, **64**, 1064-1081 (2013).

[14] Pech-May N. W., Mendioroz A., & Salazar A., "Simultaneous measurement of the in-plane and in-depth thermal diffusivity of solids using pulsed infrared thermography with focused illumination", NDT & E International, **77**, 28-34 (2016).

[15] Bamford M., Batsale J. C., & Fudym O. (2007). "Différentes stratégies pour l'estimation de profils de diffusivités thermiques d'une éprouvette composite SiCf/SiC après un flash", Congrès SFT, Île des Embiez (2007).

ACCEPTED PAPER

[16] Cernuschi F., Russo A., Lorenzoni L., & Figari A., “In-plane thermal diffusivity evaluation by infrared thermography”, Review of Scientific Instruments, **72**(10), 3988-3995 (2001).
[17] Philippi I., Batsale J. C., Maillet D., & Degiovanni A., “Measurement of thermal diffusivities through processing of infrared images”, Review of Scientific Instruments, **66**(1),182-192 (1995).
[18] Hadisaroyo D., Batsale J.C. and Degiovanni A., “Un appareillage simple pour la mesure de la diffusivité thermique de plaques minces”, Journal de Physique III, **2**, 1, 111–128 (1992).
[19] Cifuentes Á., Mendioroz A., & Salazar A., “Simultaneous measurements of the thermal diffusivity and conductivity of thermal insulators using lock-in infrared thermography”, International Journal of Thermal Sciences, **121**, 305-312 (2017).
[20] Drach V., Wiener M., Reichenauer G., Ebert H. P., & Fricke J., “Determination of the Anisotropic Thermal Conductivity of a Carbon Aerogel–Fiber Composite by a Non-contact Thermographic Technique”, International Journal of Thermophysics, **28**(5), 1542-1562 (2007).
[21] Salazar A., Mendioroz A., & Fuente R., “The strong influence of heat losses on the accurate measurement of thermal diffusivity using lock-in thermography”, Applied Physics Letters, **95**(12), 121905 (2009).
[22]Mendioroz A., Fuente-Dacal R., Apiñaniz E., & Salazar A., “Thermal diffusivity measurements of thin plates and filaments using lock-in thermography”. Review of Scientific Instruments”, **80**(7), 074904 (2009).
[23] Souhar Y., Rémy B., & Degiovanni A., “Thermal characterization of anisotropic materials at high temperature through integral methods and localized pulsed technique”, International Journal of Thermophysics, **34**(2), 322-340 (2013).
[24] Jannot Y. and Degiovanni A., “Thermal properties measurement of materials”, ISTE and Wiley editions, ISBN 978-1-78630-255-7, (2018).
[25] Marquardt D.W., “An algorithm for least-squares estimation of nonlinear parameters,” Journal of the Society for Industrial and Applied Mathematics, **11**, 2, 431-441 (1963).
[26] Beck J.V. and Arnold K.J., “Parameter Estimation in Engineering and Science”, Wiley (New York) (1977).
[27] Maillet D., Jannot Y ., Degiovanni A., “Analysis of the estimation error in a parsimonious temperature-temperature characterization technique”, International Journal of Heat and Mass Transfer, **62**, 230-241 (2013).
[28] Collishaw P.G. and Evans J.R.G., “An assessment of expressions for the apparent thermal conductivity of cellular materials”, Journal of Materials Science, **29**, 2661-2273 (1994).
[29] McAdams W.H., “Heat transmission”, 3d ed., McGraw-Hill Book Company, New York (1954).
[30] M. Schaller, X. Buffat, “Viscosité de l’air”, Available: https://documents.epfl.ch/users/m/ms/mschalle/www/.../B3.pdf. Accessed April 4, (2018).

ACCEPTED PAPER